Received: 17 January 2023 | Revised: 29 June 2023 | Accepted: 28 July 2023

DOI: 10.1002/rnc.6933

RESEARCH ARTICLE

WILEY

On the sample complexity of observers for unknown linear systems with biased dynamics estimations

Xuda Ding[1] | **Han Wang**[2] | **Jianping He**[1] | **Cailian Chen**[1] | **Xinping Guan**[1]

[1]The Department of Automation, Shanghai Jiao Tong University, Shanghai, China

[2]The Department of Engineering Science, University of Oxford, Oxford, UK

Correspondence
Jianping He, the Department of Automation, Shanghai Jiao Tong University, Minhang District, Shanghai, 200240, China.
Email: jphe@sjtu.edu.cn

Funding information
National Natural Science Foundation of China, Grant/Award Number: 61973218

Abstract

Observers have broad applications in power systems, whereas observer models are hard to obtain when the system is unknown. This article considers the observer design problems for unknown noisy linear time-invariant systems based on biased dynamics estimations. Unlike the unbiased methods, biased methods have stronger generalization ability, which benefits obtaining stable estimations for noisy systems. However, the biased estimation's influence on observer design still needs to be investigated. To analyze the influence, we exploit the impact of estimation bias-variance trade-off to observer design. Specifically, we propose a support vector regression (SVR) based estimator to provide biased estimations for the system identification of unknown linear systems. The sample complexity results of SVR with bias-variance trade-offs are analyzed and used for observer design and performance analysis. Then, a stable observer gain design algorithm is developed based on biased estimation. The observation performance is evaluated by the mean square observation error, which is shown to be adjustable by tuning the trade-off between bias and variance, thus achieving higher scalability than the unbiased methods. Finally, observing performance analysis demonstrates the influence of the bias-variance trade-off for the observer. Extensive simulation validations are conducted to verify the computed estimation error and performance optimality with different bias-variance trade-offs and noise settings.

KEYWORDS

linear systems, observers design, robust control, support vector regression, system identification

1 | INTRODUCTION

Observers have broad applications in power systems, such as transient stabilization and fault detection.[1,2] The fundamental knowledge for the design of state observers is the parameters of system dynamics. It is difficult to design an observer when the parameters are unknown. An efficient way to obtain the dynamics is parameter estimation.[3,4] Estimation procedures use input and output data to estimate system parameters, also called data-driven modeling methods. Several methods have been proposed in the past decades. System identification methods such as prediction error, instrumental

ABBREVIATIONS: LTI, linear time-invariant; MIMO, multiple-input and multiple-output; OLS, ordinary least square; SLS, system-level synthesis; SVR, support vector regression.

variable, and subspace model identification methods are proposed to estimate the state-space model directly.[5-8] Another technique to estimate the system dynamics is the adaptive observer design, which provides estimation error bound and shows promising results under the assumption that the system state matrix is in an observer canonical form.[9-11]

With the development of artificial intelligence and machine learning techniques, artificial neural networks-based modeling[12,13] and support vector machines-based modeling[14,15] have been proposed. Recently, thanks to the abilities of self-learning and adaptability, the adaptive dynamic programming-based methods based on reinforcement learning have demonstrated the capability to find the optimal control policy and practically solve the Bellman equation.[16-18] These methods can obtain near-accurate estimation to some extent, in the sense of asymptotic convergence,[5,19] minimum risks.[20,21] Also, some work obtained the estimation error bounds under strict assumptions, such as the state matrix is observable canonical form and the number of samples for identification is infinite.[9-11] However, when the number of sample is finite and state matrix is not an observable canonical form, the aforementioned studies cannot provide estimation error bounds.

More recently, it has been proposed to use finite samplings instead.[22-24] These methods are more practical since the infinite samples are hard to obtain. They also do not rely on an observable canonical form. Recent works in the control community discussed the nonasymptotic analysis and obtained a bound of bias for the dynamics estimation problem under finite samples.[23-31] Based on the ordinary least square (OLS) estimator, these works considered the Gaussian process estimation of a linear time-invariant (LTI) system. The principal tool used in the nonasymptotic regression bound analysis is concentration inequalities. The convergence rate of regression error is $\mathcal{O}(1/\sqrt{N})$, where N is the number of samples (sample length) used for regression. A line of recent works has obtained similar results for both stable and unstable systems by different data collection procedures. Based on these results, the robust controller design problem is further considered, which explores the relationships among data, estimation error, and controller performance.[22-24] Specifically, they connected the sub-optimal control cost with the regression error based on the parameterization methods such as system-level synthesis (SLS),[32] and input-output parameterization.[33,34] These works showed that it obtains tighter error bounds and better control performance with more data used for OLS regression. These methods obtained error bounds based on the sample length without considering the impact of the variance of the estimation error. An ideal estimator should be unbiased and have low variance. Since a larger estimation variance would cause more uncertainty in regression results, the variance greatly impacts stable observer design.

Moreover, machine learning methods such as neural networks[35] and support vector machines[36] can provide biased but low-variance regression results for a noisy system, Furthermore, they showed strong generalization abilities, and stability.[37] This characteristic makes machine learning methods popular in practice. The bias of the estimation fluctuates moderately. The fluctuation of bias causes the shift of the error interval. Then, it is difficult to design a robust observer when the error interval shifts. Besides, trading off the bias and variance provides flexible error bounds, which could benefit the stable observer design.

Inspired by the previous studies, this article aims to formulate and analyze the sample complexity and observer design based on the biased dynamics estimation and explore the impact of the biased results on the observer design. However, designing a stable observer gain over an unknown system with biased estimators takes work. The challenges are: (1) since there is uncertainty in biased estimation with the bias-variance trade-off, it is challenging to design a stable and robust observer gain; (2) the relationship between the designed observer performance and the biased estimation is unknown; (3) how to apply an estimation method with bias-variance trade-off to the observer design needs to be determined. To deal with these challenges, we first formulate the uncertainty in estimation based on system input and output data. Then we proposed a procedure to design a robust and stable observer based on the eigenvalue estimation of the observer state matrix. After that, the observer performance defined by the mean square observation error is analyzed with the estimation uncertainty based on SLS. Finally, the Support Vector Regression (SVR) technique is used for estimation. The estimation error bounds with bias-variance trade-offs based on finite data samples are formulated using nonasymptotic analysis. Moreover, we show that the estimator with bias-variance trade-off has higher scalability beyond the unbiased estimator in observer design with finite samples.

The main contributions of this article are threefold:

- An unknown linear system is estimated with a biased estimator (SVR) and the sample complexity bounds are obtained with the bias-variance trade-off parameter γ. The proposed estimator provides higher flexibility for stable observer design.
- The robust observer gain is designed to guarantee stability based on the estimation error bounds. It is shown that the adjustable estimation helps find a stable gain under noise and the proposed estimator is beneficial for designing a robust observer for an unknown system.

TABLE 1 Symbols and quantities.

Symbol	Definition
$\boldsymbol{A} \in \mathbb{R}^{n\times n}$	The state matrix
$\boldsymbol{B} \in \mathbb{R}^{n\times m}$	The input matrix
$\boldsymbol{C} \in \mathbb{R}^{n\times n}$	The output matrix
$\tilde{\boldsymbol{A}} \in \mathbb{R}^{n\times n}$	The estimation of state matrix
$\tilde{\boldsymbol{B}} \in \mathbb{R}^{n\times m}$	The estimation of input matrix
$\Delta\boldsymbol{A} \in \mathbb{R}^{n\times n}$	$\|\|\boldsymbol{A} - \tilde{\boldsymbol{A}}\|\|$
$\Delta\boldsymbol{B} \in \mathbb{R}^{n\times m}$	$\|\|\boldsymbol{B} - \tilde{\boldsymbol{B}}\|\|$
$\boldsymbol{x}_k \in \mathbb{R}^n$	The state at time k
$\boldsymbol{y}_k \in \mathbb{R}^n$	The output at time k
$\boldsymbol{u}_k \in \mathbb{R}^m$	The input at time k
$\boldsymbol{w}_k \sim \mathcal{N}(0, \sigma_w^2\boldsymbol{I}_n)$	The process noise
$\boldsymbol{v}_k \sim \mathcal{N}(0, \sigma_v^2\boldsymbol{I}_n)$	The measurement noise
$\boldsymbol{e}_k$	The observer error at time k
$\gamma > 0$	The parameter for bias-variance trade-off
$\boldsymbol{L} \in \mathbb{R}^{n\times n}$	The designed observer gain
$\boldsymbol{K} \in \mathbb{R}^{n\times n}$	The optimal observer gain
J	The mean square observation error
T_0	The end-time of each roll-out
N	The number of roll-outs
M	The upper bound of $\|\|\boldsymbol{A}\|\|$ and $\|\|\boldsymbol{B}\|\|$
$\mathcal{B}(c, r)$	The interval of the estimation error, where c is the center, $c - r$ and $c + r$ are the bounds

- The optimality of the designed observer is analyzed. The mean squared observation error bounds are only related to the upper bound of the estimation error. Moreover, a condition for choosing a suitable observation method is obtained to determine whether it is worth designing an observer based on dynamics estimations.

The article is organized as follows: The considered problem setting and the observer design goal are shown in Section 2. The nonasymptotic analysis and estimation error bounds based on SVR are given in Section 3. In Section 4, we propose a stable observer gain design procedure based on estimation with a bias-variance trade-off for an unknown LTI system. The performance of the designed observer of the unknown LTI system is formulated in Section 5. The numerical simulations are conducted in Section 6, to verify the proposed theoretical results both in dynamics estimation and observer design. Finally, conclusions and future research directions are given in Section 7.

Notation. We let bold symbols denote the vectors and matrices. $\boldsymbol{I}_n$ is the n-dimension identity matrix. $\|\cdot\|$ is the Euclidean norm. The $\mathcal{H}_2$ norm is defined by $\|\Phi\|_{\mathcal{H}_2}^2 \triangleq \sum_{t=0}^{\infty}\|\Phi_t\|_F^2$, where $\Phi = \sum_{t=0}^{\infty}\Phi_t z^{-1}$ is the frequency representation of signals and $\|\cdot\|_F$ is the Frobenius norm. The $\mathcal{H}_\infty$ norm is defined by $\|\Phi\|_{\mathcal{H}_\infty} \triangleq \sup_{\|z\|=1}\|\Phi(z)\|$. $\frac{1}{z}\mathcal{RH}_\infty$ is the set of real rational stable strictly proper transfer matrices. Notations $<$, $\leq$, $>$ and $\geq$ are element-wise inequality. $\mathbb{E}$ and $\mathbb{V}$ stand for the expectation and covariance, respectively. Table 1 shows some important definitions used in this article. Moreover, we refer to "estimator" for the estimation of the system dynamics and "observer" for the observation of the state.

2 | PROBLEM SETUP

We consider the multiple-input and multiple-output (MIMO) LTI system

$$\boldsymbol{x}_{k+1} = \boldsymbol{A}\boldsymbol{x}_k + \boldsymbol{B}\boldsymbol{u}_k + \boldsymbol{w}_k, \tag{1a}$$

$$\boldsymbol{y}_k = \boldsymbol{C}\boldsymbol{x}_k + \boldsymbol{v}_k, \tag{1b}$$

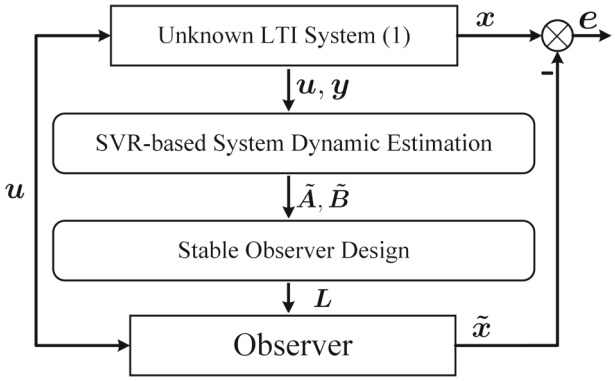

FIGURE 1 The overview of the proposed estimation and observer design synthesis.

The system is called "unknown system" for the state and input matrices are unknown. Specifically, the orders of the $\boldsymbol{A}$ and $\boldsymbol{B}$ are known, $\boldsymbol{C}$, $\boldsymbol{D}$ and the distributions of the process noise and the measurement noise are known. The elements in the matrices $\boldsymbol{A}$ and $\boldsymbol{B}$ are unknown. Throughout this article, we make the following assumption.

Assumption 1. $\boldsymbol{C}$ is invertible, $(\boldsymbol{A}, \boldsymbol{C})$ is observable, $(\boldsymbol{A}, \boldsymbol{B})$ is stabilizable, and matrices are bounded by $\|\boldsymbol{A}\|, \|\boldsymbol{B}\| \leq M$ with $M > 0$.

The matrix $\boldsymbol{C}$ is a square matrix in this study, that is, the number of states and outputs are equal. There are many power systems can be modeled as the proposed model, such as synchronous machines[38] and wind power plants.[39] Assumption 1 defines the LTI system as controllable and observable, which is a standard condition for observer design. A similar assumption is also used in the References 26 and 29. In practice, we often encounter designing an observer or Kalman filter for an unknown dynamics system. Without the dynamics, the observations are hard to obtain. When $\boldsymbol{C}$ is full-rank and known, one way to observe $\boldsymbol{x}_k$ is using $\boldsymbol{C}^{-1}\boldsymbol{y}_k$ instead of an observer. We will give a condition for choosing a better method considering reducing the noise impact in Sections 3 and 5. The scheme of the proposed estimation and observer design synthesis is shown in Figure 1. The proposed method can be used for designing a Kalman filter for an inertial measurement unit without knowing the accurate system model.

2.1 | Estimation with bias-variance trade-off

This article introduces the biased estimations of $\tilde{\boldsymbol{A}}$ and $\tilde{\boldsymbol{B}}$ with a bias-variance trade-off, based on samplings of $\boldsymbol{u}_k$ and $\boldsymbol{y}_k$. The biased results are more flexible than the unbiased ones, which can be obtained by learning methods.[35,36] We first define a trade-off parameter $\gamma > 0$, which quantifies the biased estimation error. The estimation error is defined as $\Delta\boldsymbol{A} = \boldsymbol{A} - \tilde{\boldsymbol{A}}$ and $\Delta\boldsymbol{B} = \boldsymbol{B} - \tilde{\boldsymbol{B}}$.

Definition 1 (bias-variance trade-off parameter). Given $\mathcal{H}_A \geq 0$ and $\mathcal{H}_B \geq 0$, $\gamma > 0$ is defined as a bias-variance trade-off parameter if γ satisfies

$$\frac{1}{1+\gamma}\|\gamma\tilde{\boldsymbol{A}}_i - \Delta\boldsymbol{A}_i\| \leq \mathcal{H}_A, \tag{2}$$

$$\frac{1}{1+\gamma}\|\gamma\tilde{\boldsymbol{B}}_i - \Delta\boldsymbol{B}_i\| \leq \mathcal{H}_B, \tag{3}$$

where subscript i stands for the ith row of the matrix.

Note that the trade-off parameter does not always exist, it depends on the data-driven estimation method. For example, when using the OLS to estimate the dynamics, the estimation result is an unbiased one, and $\gamma = 0$, $\|\Delta\boldsymbol{A}_i\| \leq \mathcal{H}_A$ and $\|\Delta\boldsymbol{B}_i\| \leq \mathcal{H}_B$. The center of the error interval is zero. Then, conditions (2)–(3) do not hold. When $\gamma \neq 0$, the center of the error interval is not zero, which follows the definition of biased estimation. In application, the bias-variance trade-off parameter γ is first determined, then a specific estimation method is used for estimating $\tilde{A}, \tilde{B}$. The error bounds $\mathcal{H}_A$ and $\mathcal{H}_B$ are obtained according to the specific estimation method. The key to guarantee the standing of (2)–(3) is quantifing

suitable the error bounds. This article gives the error bounds when estimating the dynamics with biased estimation method (SVR) in Section 5. To use an unbiased estimation method to obtain the error bound, we direct the reader to References 23,24,26-30. When estimating a system whose noise variance is large, a biased estimation will provide a smaller error variance than an unbiased one.[36,40] Detailed discussion about biased estimation will be given in Section 5. The term $\frac{1}{1+\gamma}$ avoids the inequalities from being infinite when $\gamma \to \infty$.

2.2 | Observer design

After estimating system dynamics, the observer gain $\boldsymbol{L}$ is designed. The observer that designed based on estimation results $\tilde{\boldsymbol{A}}$ and $\tilde{\boldsymbol{B}}$ is shown as

$$\tilde{\boldsymbol{x}}_{k+1} = \tilde{\boldsymbol{A}}\tilde{\boldsymbol{x}}_k + \tilde{\boldsymbol{B}}\boldsymbol{u}_k + \boldsymbol{L}(\boldsymbol{y}_k - \boldsymbol{C}\tilde{\boldsymbol{x}}_k). \tag{4}$$

Then, the observer error $\boldsymbol{e}_k = \tilde{\boldsymbol{x}}_k - \boldsymbol{x}_k$ can be written as

$$\boldsymbol{e}_{k+1} = (\boldsymbol{A} - \boldsymbol{LC})\boldsymbol{e}_k - \Delta\boldsymbol{A}\tilde{\boldsymbol{x}}_k - \Delta\boldsymbol{B}\boldsymbol{u}_k - \boldsymbol{w}_k + \boldsymbol{L}\boldsymbol{v}_k, \tag{5}$$

where $\boldsymbol{L} \in \mathbb{R}^{n\times p}$ is the observer gain, which is also used in the Kalman filter and linear quadratic Gaussian control design. $\tilde{\boldsymbol{x}}_k \in \mathbb{R}^n$ is the state given by the observer.

Apparently, $\boldsymbol{L}$ needs to be designed so that $\boldsymbol{A} - \boldsymbol{LC}$ is stable. When $\boldsymbol{A}$ is known, it is easy to design a suitable $\boldsymbol{L}$ and make the spectrum radius $\rho(\boldsymbol{A} - \boldsymbol{LC}) < 1$ and the observer be stable. Moreover, a well-designed $\boldsymbol{L}$ can filter the noise in (5). By referring to Reference 22, we use the mean square observation error J to measure the observer performance,

$$J = \sqrt{\lim_{T\to\infty}\left(\frac{1}{T}\sum_{k=0}^{T}\|\boldsymbol{e}_{k+1}\|^2\right)}. \tag{6}$$

The value of J depends on the dynamics estimation results and designed observer gain. The two-step procedure, estimation and observer application, give the end-to-end performance analysis based on unbiased estimation,[22-24] which shows that the cost depends on the N data sampled. When $N \to \infty$, $\|\Delta\boldsymbol{A}\| \to 0$ and $\|\Delta\boldsymbol{B}\| \to 0$, and optimal $\boldsymbol{L}$ can be designed to make the cost is 0.[41]

However, when the biased dynamics estimation based on finite data is used for $\boldsymbol{L}$ design, the uncertainty in determining $\rho(\boldsymbol{A} - \boldsymbol{LC})$ needs to be considered. Moreover, the impact of the biased estimation on the observer performance needs to be investigated since the trade-off parameter γ brings scalability to estimation.

3 | SVR ESTIMATION ERROR BOUND ANALYSIS

In this section, we use the SVR method to estimate the system (1) and obtain the biased estimations. Moreover, the parameter γ is used in SVR to trade off the bias and variance.

3.1 | Data collection

Since we do not assume that the system (1) is open-loop stable, the output variable $\boldsymbol{y}$ might blow up during the data collection process. Inspired by previous study on OLS regression,[23,24,26-30] we use multi-roll-out procedure to collect $\boldsymbol{u}_k$ and $\boldsymbol{y}_k$. The essence of this procedure is to use collected data in a finite time horizon. The system with $\boldsymbol{x}_0 = 0$ is excited by Gaussian input $\boldsymbol{u}_k \sim \mathcal{N}(0, \sigma_u^2\boldsymbol{I}_m)$. The data set is then recorded as

$$\left\{\left(\boldsymbol{y}_k^i, \boldsymbol{u}_k^i\right) : 1 \le i \le N, 0 \le k \le T_0\right\}, \tag{7}$$

where i is the index for each roll-out, and T_0 is the end time of the roll-out. The total number of data points is NT_0. Gaussian input satisfies the sufficient persistency of excitation condition for linear systems.[42] A similar roll-out procedure is used

in References 23,24,27 to deal with unstable single-input single-output, and MIMO systems. Besides multiple roll-out procedures, single roll-out procedures are used to identify open-loop stable systems.[26,28-30]

Remark 1. $\boldsymbol{x}_0$ can follow a Gaussian distribution with finite variance, which does not influence the regression procedure and regression error analysis.[24]

3.2 | SVR procedure

After data collection, an SVR-based estimator is used to estimate the system dynamics. Input and output data are put into tuples for each roll-out,

$$f(\boldsymbol{z}_k) = \left[\boldsymbol{y}_k^1, \boldsymbol{y}_k^2, \dots, \boldsymbol{y}_k^N\right] \in \mathbb{R}^{n\times N}, \tag{8a}$$

$$\boldsymbol{z}_k = \begin{bmatrix} \boldsymbol{y}_{k-1}^1, & \boldsymbol{y}_{k-1}^2, \dots, & \boldsymbol{y}_{k-1}^N \\ \boldsymbol{u}_{k-1}^1 & \boldsymbol{u}_{k-1}^2 & \boldsymbol{u}_{k-1}^N \end{bmatrix} \in \mathbb{R}^{(n+m)\times N}, \tag{8b}$$

and the noises $\boldsymbol{w}$ and $\boldsymbol{v}$ are represented as

$$\boldsymbol{b}_k = \left[\boldsymbol{w}_{k-1}^1 + \boldsymbol{v}_k^1 - \boldsymbol{A}\boldsymbol{v}_{k-1}^1, \dots, \boldsymbol{w}_{k-1}^N + \boldsymbol{v}_k^N - \boldsymbol{A}\boldsymbol{v}_{k-1}^N\right]. \tag{9}$$

Combine all the data as

$$\mathcal{D}_k = [f(\boldsymbol{z}_k); \boldsymbol{z}_k; \boldsymbol{b}_k] \in \mathbb{R}^{(3n+m)\times N}. \tag{10}$$

When $k = T_0$, the final data is used to estimate system dynamics, and such a procedure is called final-data estimation.[23,27] The number of rounds in the final data collection is N, and all data is recorded. To efficiently use the data collected in the collection procedure, data from $k = 1$ to $k = T_0$ are all used for estimation, as $\{\mathcal{D}_1, \mathcal{D}_2, \dots, \mathcal{D}_{T_0}\} \in \mathbb{R}^{(3n+m)\times(T_0-1)N}$. This procedure is referred to as all-data estimation.

Unlike OLS, which can estimate the coefficients of a matrix at one time, ordinary SVR can only regress one row of a matrix. To ease the notation, we consider the estimation based on $\mathcal{D}_{T_0}$ in the following subsection. Then, regression of (1a) for each row of $\left[\boldsymbol{C}^{-1}\boldsymbol{A},\ \boldsymbol{C}^{-1}\boldsymbol{B}\right]$ is shown as

$$f_i(\boldsymbol{z}_k) = \left[\boldsymbol{C}^{-1}\boldsymbol{A},\ \boldsymbol{C}^{-1}\boldsymbol{B}\right]_i \boldsymbol{z}_k + \boldsymbol{b}_{k,i}, \tag{11}$$

where subscript i stands for the ith row of the matrix, that is, $f_i(\boldsymbol{z}_k) \in \mathbb{R}^{1\times N}$, $\left[\boldsymbol{C}^{-1}\boldsymbol{A},\ \boldsymbol{C}^{-1}\boldsymbol{B}\right]_i \in \mathbb{R}^{1\times(n+m)}$, $\boldsymbol{b}_{k,i} \in \mathbb{R}^{1\times N}$. For clear expression, we denote $\left[\boldsymbol{C}^{-1}\boldsymbol{A},\ \boldsymbol{C}^{-1}\boldsymbol{B}\right]$ as $\left[\hat{\boldsymbol{A}},\ \hat{\boldsymbol{B}}\right]$.

$$\min_{[\hat{\boldsymbol{A}},\ \hat{\boldsymbol{B}}]_i} \mathcal{L}_i = \frac{1}{2}\left\|\left[\hat{\boldsymbol{A}},\ \hat{\boldsymbol{B}}\right]_i\right\|^2 + \frac{1}{2\gamma}\sum_{j=1}^{N}(\xi_j^{+2} + \xi_j^{-2}), \tag{12a}$$

$$\text{s.t. } f_i(\boldsymbol{z}_k^j) - \left[\hat{\boldsymbol{A}},\ \hat{\boldsymbol{B}}\right]_i \boldsymbol{z}_k^j - \xi_j^+ \le 0, \tag{12b}$$

$$-f_i(\boldsymbol{z}_k^j) + \left[\hat{\boldsymbol{A}},\ \hat{\boldsymbol{B}}\right]_i \boldsymbol{z}_k^j - \xi_j^- \le 0, \tag{12c}$$

$$\xi_j^+, \xi_j^- \ge 0, \tag{12d}$$

where $\boldsymbol{z}_k^j \in \mathbb{R}^{(n+m)\times 1}$ is the jth column of $\boldsymbol{z}_k$, $f_i(\boldsymbol{z}_k^j) \in \mathbb{R}$, ξ_j^+ and ξ_j^- are slack variables to separate $\boldsymbol{b}_{k,i}^j \ge 0$ and $\boldsymbol{b}_{k,i}^j \le 0$. γ is the parameter. Although the estimation results cannot be identical to the actual value due to the noise, the estimation goal in this article is to get a bounded deviation-based finite sample. The estimations of $\boldsymbol{A}$ and $\boldsymbol{B}$ are given based on solving the dual problem of (12) by introducing non-nagetive dual parameter $\boldsymbol{\alpha} \in \mathbb{R}^{N\times 1}$ as

$$\left[\boldsymbol{C}^{-1}\tilde{\boldsymbol{A}},\ \boldsymbol{C}^{-1}\tilde{\boldsymbol{B}}\right]_i = \boldsymbol{\alpha}^\top \boldsymbol{z}_k^\top, \tag{13}$$

where $\tilde{\boldsymbol{A}}$ and $\tilde{\boldsymbol{B}}$ are the estimations of $\boldsymbol{A}$ and $\boldsymbol{B}$, respectively. We refer readers to Reference 43 for the details about obtaining (13). The augmented SVR is formulated to estimate $\boldsymbol{A}$ and $\boldsymbol{B}$,

$$\arg\min_{[\hat{\boldsymbol{A}},\,\hat{\boldsymbol{B}}]} \sum_{i=1}^{n} \mathcal{L}_i. \tag{14}$$

Note that the parameter γ can be used to trade off bias and variance of the estimation.[36] When $\gamma \to 0$, the second term of (12a) dominates the minimization, and the estimation results tend to be the same as the unbiased results of OLS. The variance of the estimation decreases as parameter γ increases. These methods attempt to decrease the regression variance and improve the model's robustness by sacrificing the unbiasedness property. However, OLS seeks to obtain an unbiased estimation and overlooks the variance, which could lead to poor performance (i.e., large variance) in regression. Thus, compared to OLS, we can use SVR with a tunable parameter γ to control the trade-off between bias and variance and improve the estimation performance.

3.3 | Sample complexity of the SVR estimation

We first show the distribution of SVR estimation for an LTI Gaussian system. Define the matrices $\boldsymbol{G}_k$ and $\boldsymbol{F}_k$ as

$$\boldsymbol{G}_k = \begin{bmatrix} \boldsymbol{A}^{k-1}\boldsymbol{B} & \boldsymbol{A}^{k-2}\boldsymbol{B} & \dots & \boldsymbol{B} \end{bmatrix},$$

$$\boldsymbol{F}_k = \begin{bmatrix} \boldsymbol{A}^{k-1} & \boldsymbol{A}^{k-2} & \dots & \boldsymbol{I}_n \end{bmatrix}.$$

Then, $f\left(\begin{bmatrix} \boldsymbol{y}_{k-1} \\ \boldsymbol{u}_{k-1} \end{bmatrix}\right)$ and $\begin{bmatrix} \boldsymbol{y}_{k-1} \\ \boldsymbol{u}_{k-1} \end{bmatrix}$ follow

$$f\left(\begin{bmatrix} \boldsymbol{y}_{k-1} \\ \boldsymbol{u}_{k-1} \end{bmatrix}\right) \sim \mathcal{N}(0, \boldsymbol{\sigma}_k^2),$$

$$\begin{bmatrix} \boldsymbol{y}_{k-1} \\ \boldsymbol{u}_{k-1} \end{bmatrix} \sim \mathcal{N}\left(0, \begin{bmatrix} \boldsymbol{\sigma}_{k-1}^2 & 0 \\ 0 & \sigma_u^2 \boldsymbol{I}_m \end{bmatrix}\right),$$

where $\boldsymbol{\sigma}_k^2 = \sigma_u^2 \boldsymbol{G}_k \boldsymbol{G}_k^\top + \left(\sigma_w^2 + \sigma_v^2\right)\boldsymbol{F}_k \boldsymbol{F}_k^\top + \sigma_v^2 \boldsymbol{F}_{k+1} \boldsymbol{F}_{k+1}^\top$. Notice that the noise will propagate throughout the system with time, and the accumulation is directly reflected by convolution, which is represented by $\boldsymbol{G}_k$ and $\boldsymbol{F}_k$. By Assumption 1, we have $\|\boldsymbol{A}\| \le M$ and $\|\boldsymbol{B}\| \le M$, thus $\mathbb{V}(\boldsymbol{B}\boldsymbol{u}_k) \le mM\sigma_u^2 \boldsymbol{I}_n$ and $\boldsymbol{\sigma}_k^2 \le (nM^{2T_0-1}\sigma_u^2 + M^{2T_0-2}(\sigma_w^2 + \sigma_v^2) + M^{2T_0}\sigma_v^2)\boldsymbol{I}_n$ when $k = T_0$. Then, the regression procedure can be considered into two parts: i) regressing $\boldsymbol{A}$ with the residual terms $\boldsymbol{B}\boldsymbol{u}_{T_0}$ and $\boldsymbol{w}_{T_0} + \boldsymbol{v}_{T_0+1} - \boldsymbol{A}\boldsymbol{v}_{T_0}$, which can be treated as the noise together. Since $\mathbb{V}(\boldsymbol{B}\boldsymbol{u}_k) \le mM\sigma_u^2 \boldsymbol{I}_n$ and $\mathbb{V}(\boldsymbol{w}_{T_0} + \boldsymbol{v}_{T_0+1} - \boldsymbol{A}\boldsymbol{v}_{T_0}) \le (\sigma_w^2 + (M+1)\sigma_v^2)\boldsymbol{I}_n$, the covariance of the noise when regressing $\boldsymbol{A}$ is equal or less than $\sigma_A^2 \boldsymbol{I}_n = (mM\sigma_u^2 + \sigma_w^2 + (M+1)\sigma_v^2)\boldsymbol{I}_n$. ii) regressing $\boldsymbol{B}$ with the residual terms $\boldsymbol{A}\boldsymbol{y}_{T_0}$ and $\boldsymbol{w}_{T_0} + \boldsymbol{v}_{T_0+1} - \boldsymbol{A}\boldsymbol{v}_{T_0}$, which can be treated as the noise together. Since $\boldsymbol{\sigma}_{T_0}^2 \le (nM^{2T_0-1}\sigma_u^2 + M^{2T_0-2}\sigma_w^2)\boldsymbol{I}_n$ and $\mathbb{V}(\boldsymbol{w}_{T_0} + \boldsymbol{v}_{T_0+1} - \boldsymbol{A}\boldsymbol{v}_{T_0}) \le (\sigma_w^2 + (M+1)\sigma_v^2)\boldsymbol{I}_n$, the covariance of the noise when regressing $\boldsymbol{B}$ is equal or less than $\sigma_B^2 \boldsymbol{I}_n = (nM^{2T_0-1}\sigma_u^2 + (M^{2T_0-2}+1)\sigma_w^2 + (M+1)\sigma_v^2)\boldsymbol{I}_n$.

Lemma 1. *For a linear system with independent Gaussian noise (1a), the expectation and variance of $\tilde{\boldsymbol{A}}_i$ estimated by SVR with L_2 loss (14) are*

$$\mathbb{E}(\tilde{\boldsymbol{A}}_i) = \frac{1}{1+\gamma}\boldsymbol{A}_i, \tag{15a}$$

$$\mathbb{V}(\tilde{\boldsymbol{A}}_i) \le \frac{1}{1+\gamma}(\sigma_A^2(\boldsymbol{y}_{T_0-1}\boldsymbol{y}_{T_0-1}^\top)^{-1} + \gamma M^2 \boldsymbol{I}_n), \tag{15b}$$

and the expectation and the variance of $\tilde{\boldsymbol{B}}_i$

$$\mathbb{E}(\tilde{\boldsymbol{B}}_i) = \frac{1}{1+\gamma}\boldsymbol{B}_i, \tag{16a}$$

$$\mathbb{V}(\tilde{\boldsymbol{B}}_i) \le \frac{1}{1+\gamma}(\sigma_B^2(\boldsymbol{u}_{T_0-1}\boldsymbol{u}_{T_0-1}^\top)^{-1} + \gamma M^2 \boldsymbol{I}_m), \tag{16b}$$

Proof. Please see Appendix A.1. ∎

Note that $\sigma_A^2(\boldsymbol{y}_{T_0-1}\boldsymbol{y}_{T_0-1}^\top)^{-1}$ is the estimation variance based on OLS. Thus SVR has a $\mathcal{O}(1/(1+\gamma))$ minor estimation error variance under more considerable variance noise (see Appendix A.1). Thus, SVR can provide more stable results than OLS when estimating a system with large noise. Since there is a linear relationship between OLS-based estimation and SVR-based one, the estimation results of SVR follow a normal distribution. Moreover, when only the upper bound of the process and measurement noise variances are known, the upper bound of σ_A^2 and σ_B^2 can be deduced with the procedure mentioned above.

The distribution of $\tilde{\boldsymbol{A}}_i$ and $\tilde{\boldsymbol{B}}_i$ cannot be used to quantify the error bound with a certain value. Then, Theorem 1 is given to quantify the estimation error bound.

Theorem 1. *Given a constant $\delta \in (0,1)$. If all-data in N roll-outs from beginning to T_0 is used for estimation based on SVR in (14), then we have the bounds with probability at least $1-\delta$ as,*

$$\frac{1}{1+\gamma}\|\gamma\tilde{\boldsymbol{A}}_i - \Delta\boldsymbol{A}_i\| \le \sqrt{\frac{\theta_A + n\gamma M^2}{(1+\gamma)N_0}} + \sqrt{\frac{2(\theta_A + n\gamma M^2)\log(1/\delta)}{(1+\gamma)N_0}}, \tag{17}$$

$$\frac{1}{1+\gamma}\|\gamma\tilde{\boldsymbol{B}}_i - \Delta\boldsymbol{B}_i\| \le \sqrt{\frac{\theta_B + m\gamma M^2}{(1+\gamma)N_0}} + \sqrt{\frac{2(\theta_B + m\gamma M^2)\log(1/\delta)}{(1+\gamma)N_0}}, \tag{18}$$

where $N_0 = (T_0-1)N$, $\theta_A = \frac{4n(mM\sigma_u^2+\sigma_w^2+(M+1)\sigma_v^2)}{N(nM^{2T_0-1}\sigma_u^2+M^{2T_0-2}(\sigma_w^2+\sigma_v^2)+M^{2T_0}\sigma_v^2)}$ *and* $\theta_B = \frac{4m(nM^{2T_0-1}\sigma_u^2+(M^{2T_0-2}+1)\sigma_w^2+(M+1)\sigma_v^2)}{N\sigma_u^2}$.

Proof. Please see Appendix A.2. ∎

Theorem 1 formulates the relationship between the estimation and the estimation error. Different from the sample complexity of the OLS-based estimator, which directly gives the bound of the estimation error, Theorem 1 shows the bound of $\|\gamma\tilde{\boldsymbol{A}}_i - \Delta\boldsymbol{A}_i\|$ for the bias-variance trade-off in the estimation. Since $\tilde{\boldsymbol{A}}_i$ can be obtained when the training sample and sample length are given, the uncertainty of estimation error is quantified in Theorem 1. Theorem 1 also states that the sample-complexities of $\Delta\boldsymbol{A}_i$ and $\Delta\boldsymbol{B}_i$ behavior as $\mathcal{O}(1/\sqrt{N})$, which is consistent with the previous studies based on OLS estimation.[23,24,26-29] Further, the parameter γ can change the bound of estimation error under fixed sample length N. The essence lies in the bias-variance trade-off based on the parameter γ in SVR.

Based on the estimation bound given in Theorem 1, $\mathcal{H}_A$ and $\mathcal{H}_B$ are given with probability at least $1-\delta$ as,

$$\mathcal{H}_A = \sqrt{\frac{\theta_A + n\gamma M^2}{(1+\gamma)N_0}} + \sqrt{\frac{2(\theta_A + n\gamma M^2)\log(1/\delta)}{(1+\gamma)N_0}}, \tag{19a}$$

$$\mathcal{H}_B = \sqrt{\frac{\theta_B + m\gamma M^2}{(1+\gamma)N_0}} + \sqrt{\frac{2(\theta_B + m\gamma M^2)\log(1/\delta)}{(1+\gamma)N_0}}. \tag{19b}$$

This shows that the error bound $\mathcal{H}_A$ and $\mathcal{H}_B$ can be decreased by increasing γ when regressing the system (1) with large noise ($\theta_A \ge nM^2, \theta_B \ge mM^2$). Otherwise, when the noise variance is small ($\theta_A \le nM^2, \theta_B \le mM^2$), it is better to use a small parameter γ.

4 | RESULTS ON STABLE GAIN DESIGN

In this section, we introduce the design of the stable observer gain based on biased estimation. The interval of the estimation error needs to be determined to quantify the uncertainty bound. The interval of the estimation error is defined as $\mathcal{B}(c,r) = [c-r, c+r]$, where c is the center, $c-r$ and $c+r$ are the bounds.

Lemma 2. *Suppose the estimation defined in Definition 1 is given, then the estimation error of the elements of* $\boldsymbol{A}$ *and* $\boldsymbol{B}$ *are in the intervals as*

$$\Delta \boldsymbol{A}_{i,j} \in \mathcal{B}\left(\gamma \tilde{\boldsymbol{A}}_{i,j}, \sqrt{(1+\gamma)\mathcal{H}_A}\right), \tag{20a}$$

$$\Delta \boldsymbol{B}_{i,j} \in \mathcal{B}\left(\gamma \tilde{\boldsymbol{B}}_{i,j}, \sqrt{(1+\gamma)\mathcal{H}_B}\right), \tag{20b}$$

Proof. Please see Appendix A.3. ∎

Lemma 2 further illustrates that γ can change the interval of error. The bias-variance trade-off lies in the different variation rates of the center and the radius in (20). More importantly, γ can change the bound of the error interval, which provides scaleability in the uncertainty analysis. Take the estimation of $\boldsymbol{A}$ as an example. The interval of $\boldsymbol{A}$ is obtained by the estimation procedure as

$$\boldsymbol{A}_{i,j} \in \mathcal{B}\left((1+\gamma)\tilde{\boldsymbol{A}}_{i,j}, \sqrt{(1+\gamma)\mathcal{H}_A}\right). \tag{21}$$

When analyzing the stability of $\boldsymbol{A}$, the spectral radius needs to be examined. The biased estimation in (21) provides a way to adjust the asymmetric interval of $\boldsymbol{A}_{i,j}$ by tuning γ. Bounds of $||\Delta \boldsymbol{A}||$ and $||\Delta \boldsymbol{B}||$ can be obtained by the following lemma.

Lemma 3. *Suppose (20) holds true, then* $||\Delta \boldsymbol{A}|| \leq \epsilon_A$ *and* $||\Delta \boldsymbol{B}|| \leq \epsilon_B$, *where* ϵ_A *and* ϵ_B *are*

$$\epsilon_A = \sqrt{\sum_{i=1}^{n}\sum_{j=1}^{n}\left(||\gamma \tilde{\boldsymbol{A}}_{i,j}|| + \sqrt{(1+\gamma)\mathcal{H}_A}\right)^2}, \tag{22a}$$

$$\epsilon_B = \sqrt{\sum_{i=1}^{n}\sum_{j=1}^{m}\left(||\gamma \tilde{\boldsymbol{B}}_{i,j}|| + \sqrt{(1+\gamma)\mathcal{H}_B}\right)^2}. \tag{22b}$$

After estimation and obtaining the error interval, the observer gain $\boldsymbol{L}$ needs to be designed to guarantee the stability of the observer. Specifically, the goal is to determine $\boldsymbol{L}$, so that $\boldsymbol{A} - \boldsymbol{LC}$ is stable. However, only the interval of $\boldsymbol{A}$ can be obtained by the estimation procedure as (21). Then $\boldsymbol{A} - \boldsymbol{LC}$ is in the interval as

$$\boldsymbol{A}_{i,j} - \{\boldsymbol{LC}\}_{i,j} \in \mathcal{B}\left((1+\gamma)\tilde{\boldsymbol{A}}_{i,j} - \{\boldsymbol{LC}\}_{i,j}, \sqrt{(1+\gamma)\mathcal{H}_A}\right), \tag{23}$$

where $\{\boldsymbol{LC}\}_{i,j}$ is the i,jth element in $\boldsymbol{LC}$. Then, the design of stable observer gain is equivalent to finding a suitable $\boldsymbol{L}$, such that the spectral radius of the matrix $\boldsymbol{A} - \boldsymbol{LC}$ is smaller than 1. Determining the robustness of a given observer gain (or controller) under uncertainty is widely studied. Several methods are developed to infer the range of uncertainty for the robust controller.[44-46] However, designing a robust observer gain (controller) is still a hard problem.[47] A conservative design for a stable observer gain is given in Theorem 2, where $\boldsymbol{L}$ guarantees that $\boldsymbol{A} - \boldsymbol{LC}$ is stable for all combinations in (23).

Theorem 2. *Given the range of* $\boldsymbol{A}$ *in (23), if the observer is stable (i.e., the observer error is bounded), then the observer gain* $\boldsymbol{L}$ *satisfies*

$$\|\boldsymbol{A}_{i,i} - \{\boldsymbol{LC}\}_{i,j}\| < 1, \tag{24a}$$

$$\sum_{i\neq j, j=1}^{j=n} \{\|(1+\gamma)\tilde{\boldsymbol{A}}_{i,j} - \{\boldsymbol{LC}\}_{i,j}\| + \sqrt{(1+\gamma)\mathcal{H}_A}\} \leq 1 - \|\boldsymbol{A}_{i,i} - \{\boldsymbol{LC}\}_{i,j}\|. \tag{24b}$$

Proof. Please see Appendix A.4. ∎

Theorem 2 gives necessary conditions for obtaining a stable observer gain $\boldsymbol{L}$, which are valid for a general form of matrix $\boldsymbol{A}-\boldsymbol{LC}$. The observer gain can be easily designed when the uncertain system is with weakly-coupled states, that is, the norm of the diagonal element is much larger than that of the other element.

Remark 2. Equation (24a) shows that a smaller range of interval of (21) leads to finding $\boldsymbol{L}$ more easily. The range of interval $\sqrt{(1+\gamma)\mathcal{H}_A}$ depends on γ and $\mathcal{H}_A$. When $\gamma \to 0$, the estimation tends to be unbiased with a larger variance, which leads to larger $\mathcal{H}_A$. Similarly, the sum term needs to be small to satisfy the inequality in (24b). Note that the error bound is asymmetric. The center of the error bound is away from 0 as γ increases, leading to the sum term decreasing. Therefore, the trade-off in bias-variance enables selecting a suitable parameter to obtain a minimum $\sqrt{(1+\gamma)\mathcal{H}_A}$, which benefits designing a stable observer gain for an unknown system.

5 | RESULTS ON OBSERVER PERFORMANCE ANALYSIS

The observer performance is analyzed based on the observer gain designed in Section 4. First, suppose there exists an optimal observer gain $\boldsymbol{K}$, which is obtained by solving the Ricatti equation of the observer[48] and $J=0$ in (6). When the system dynamics is known, the observer error $\boldsymbol{e}(z)$ in (5) is given with z-transfer into frequency domain according to (5) in the Reference 22 as

$$(z\boldsymbol{I}-\boldsymbol{A}+\boldsymbol{LC})^{-1}\boldsymbol{K}\boldsymbol{v}-(z\boldsymbol{I}-\boldsymbol{A}+\boldsymbol{LC})^{-1}\boldsymbol{L}\boldsymbol{v}. \tag{25}$$

Notice that only the measurement noise $\boldsymbol{v}$ displays in (25) since the observer gain $\boldsymbol{K}$ has already balanced the process noise $\boldsymbol{w}$ and measurement noise $\boldsymbol{v}$. Define the noise $\boldsymbol{e}(z)$ responses to $\boldsymbol{K}\boldsymbol{v}$ and $\boldsymbol{v}$ by $\Phi_w \triangleq (z\boldsymbol{I}-\boldsymbol{A}+\boldsymbol{LC})^{-1}$ and $\Phi_v \triangleq (z\boldsymbol{I}-\boldsymbol{A}+\boldsymbol{LC})^{-1}\boldsymbol{L}$, respectively. Then, the observer error $\boldsymbol{e}(z)$ is given as

$$\boldsymbol{e}=(\Phi_w\boldsymbol{K}-\Phi_v)\boldsymbol{v}, \tag{26}$$

$\boldsymbol{L}$ is parameterized as $\Phi_w^{-1}\Phi_v$, where the closed-loop responses Φ_w and Φ_v are in the set of real rational stable strictly proper transfer matrices $\frac{1}{z}\mathcal{RH}_\infty$. When the observer is internally stable, the mean squared error is

$$J=\|(\Phi_w\boldsymbol{K}-\Phi_v)\sigma_v\|_{\mathcal{H}_2}, \tag{27}$$

where $\|\cdot\|_{\mathcal{H}_2}$ is the $\mathcal{H}_2$ norm. When $\boldsymbol{L}=\boldsymbol{K}$, the error-free observer is achieved, and $J=0$. The observer error $\boldsymbol{e}(z)$ is given as

$$\boldsymbol{e}=\tilde{\Phi}_w\Delta\boldsymbol{A}\Phi_A\boldsymbol{B}\boldsymbol{u}+\tilde{\Phi}_w\Delta\boldsymbol{A}\Phi_A\boldsymbol{K}\boldsymbol{v}+\tilde{\Phi}_w\Delta\boldsymbol{B}\boldsymbol{u}+(\tilde{\Phi}_w\boldsymbol{K}-\tilde{\Phi}_v)\boldsymbol{v}, \tag{28}$$

where $\tilde{\Phi}_w \triangleq (z\boldsymbol{I}-\tilde{\boldsymbol{A}}+\boldsymbol{LC})^{-1}$, $\tilde{\Phi}_v \triangleq (z\boldsymbol{I}-\tilde{\boldsymbol{A}}+\boldsymbol{LC})^{-1}\boldsymbol{L}$, $\Phi_A \triangleq (z\boldsymbol{I}-\boldsymbol{A})^{-1}$ and $(z\boldsymbol{I}-\boldsymbol{A})$ is inevitable. Then, the mean squared error of the state for the observer with uncertainty is given in Lemma 4.

Lemma 4. *The stable observer of system (1) has a mean squared observation error J as*

$$J=\left\|\begin{bmatrix}\tilde{\Phi}_w & \tilde{\Phi}_v\end{bmatrix}\begin{bmatrix}\boldsymbol{K}\\ -\boldsymbol{I}\end{bmatrix}\sigma_v+\tilde{\Phi}_w[\Delta\boldsymbol{A}\quad\Delta\boldsymbol{L}]\begin{bmatrix}\Phi_A\boldsymbol{K}\\ \boldsymbol{I}\end{bmatrix}\sigma_v+\tilde{\Phi}_w[\Delta\boldsymbol{A}\quad\Delta\boldsymbol{B}]\begin{bmatrix}\Phi_A\boldsymbol{B}\\ \boldsymbol{I}\end{bmatrix}\sigma_u\right\|_{\mathcal{H}_2}, \tag{29}$$

where $\Delta\boldsymbol{L}=\boldsymbol{K}-\boldsymbol{L}$ is the difference between designed observer gain and optimal gain.

The input $\boldsymbol{u}$ and noise $\boldsymbol{v}$ both influence the observer error as shown in (5). When $\boldsymbol{L}$ is designed based on Theorem 2, the upper bound of the mean squared observation error is given in the following Theorem.

Theorem 3. *Given dynamics estimation satisfies* $\|\Delta \boldsymbol{A}\| \le \epsilon_A$, $\|\Delta \boldsymbol{B}\| \le \epsilon_B$ *and* $\|\Delta \boldsymbol{L}\| \le \epsilon_L$. *The upper bound* J_1 *of the mean squared error* J *is*

$$J \le J_1(\boldsymbol{K}) = \left\|\tilde{\Phi}_w \boldsymbol{K} - \tilde{\Phi}_v\right]\right\|_{\mathcal{H}_2} \sigma_v + \sqrt{2}\epsilon_1 \left\|\tilde{\Phi}_w\right\|_{\mathcal{H}_2} \left\| \begin{bmatrix} \Phi_A \boldsymbol{B} \\ \boldsymbol{I} \end{bmatrix} \right\|_{\mathcal{H}_\infty} \sigma_u + \sqrt{2}\epsilon_2 \left\|\tilde{\Phi}_w\right\|_{\mathcal{H}_2} \left\| \begin{bmatrix} \Phi_A \boldsymbol{K} \\ \boldsymbol{I} \end{bmatrix} \right\|_{\mathcal{H}_\infty} \sigma_v, \tag{30}$$

where $\epsilon_1 = \max\{\epsilon_A, \epsilon_B\}$ *and* $\epsilon_2 = \max\{\epsilon_A, \epsilon_L\}$.

Proof. Please see Appendix A.5. ∎

The term ϵ_L is bounded since $\boldsymbol{A}$ and $\tilde{\boldsymbol{A}}$ are bounded. When directly using $\boldsymbol{C}^{-1}\boldsymbol{y}_k$ to observer $\boldsymbol{x}_k$, the observer performance is $J_{\boldsymbol{y}} = \|\boldsymbol{C}^{-1}\|\sigma_v$. Although $\boldsymbol{K}$ cannot be obtained directly, it satisfies the conditions in Theorem 2. Therefore, an alternative solution for the bound of J can be obtained as

$$\begin{aligned} J \le J_2 = \max_{\hat{\boldsymbol{K}}} \; & J_1(\hat{\boldsymbol{K}}) \\ \text{s.t. } & \hat{\boldsymbol{K}} \text{ follows (25).} \end{aligned} \tag{31}$$

Then, the following corollary is given to choose a better observation method.

Corollary 1. *Given the performance upper bound* J_2 *of (31) and* $J_y = \|\boldsymbol{C}^{-1}\|\sigma_v$, *the mean squared observation error of using observer design method is smaller than that of using direct observation method when* $J_2 < J_y$.

Corollary 1 shows that when $J_2 < J_y$, it is better to design an observer for $\boldsymbol{x}_k$ observation based on the proposed method, since (31) gives an upper bound of the mean squared observation error using observer design method. It also indicates that the key for accurate observation is that the bounds of $\|\Delta \boldsymbol{A}\|$ and $\|\Delta \boldsymbol{B}\|$ are small. The parameter γ influences the bounds and further influences the performance. Moreover, $\mathcal{H}_A$ and $\mathcal{H}_B$ also influence the performance, which will be discussed after we give a specific regression method in Section 3.

Note that the performance J can be improved by choosing an optimal $\boldsymbol{L}$. The combination of the last two terms in (30) is upper bounded by

$$\sqrt{2}\epsilon_{1,2}\left\|\tilde{\Phi}_w\right\|_{\mathcal{H}_2} \left\{ \left\| \begin{bmatrix} \Phi_A \boldsymbol{B} \\ \boldsymbol{I} \end{bmatrix} \right\|_{\mathcal{H}_\infty} \sigma_u + \left\| \begin{bmatrix} \Phi_A \boldsymbol{K} \\ \boldsymbol{I} \end{bmatrix} \right\|_{\mathcal{H}_\infty} \sigma_v \right\}, \tag{32}$$

where $\epsilon_{1,2} = \max\{\epsilon_1, \epsilon_2\}$. An alternating simplified formulation is introduced by using a robust SLS optimization technique:

$$\begin{aligned} J_{opt} = \min_{\tilde{\Phi}_w, \tilde{\Phi}_v} \; & F\left\|\tilde{\Phi}_w\right\|_{\mathcal{H}_2} + \left\|\tilde{\Phi}_w \boldsymbol{K} - \tilde{\Phi}_v\right\|_{\mathcal{H}2}, \\ \text{s.t. } & \left\|\tilde{\Phi}_w\right\|_{\mathcal{H}_2} \le C, \\ & \tilde{\Phi}_w(z\boldsymbol{I} - \tilde{\boldsymbol{A}}) - \tilde{\Phi}_v = \boldsymbol{I}, \\ & \tilde{\Phi}_w, \tilde{\Phi}_v \in \frac{1}{z}\mathcal{R}\mathcal{H}_\infty, \end{aligned} \tag{33}$$

where C is a regulation parameter to bound $\left\|\tilde{\Phi}_w\right\|_{\mathcal{H}_2}$, $F = \sqrt{2}\epsilon_{1,2}\left\{ \left\| \begin{bmatrix} \Phi_A \boldsymbol{B} \\ \boldsymbol{I} \end{bmatrix} \right\|_{\mathcal{H}_\infty} \sigma_u + \left\| \begin{bmatrix} \Phi_A \boldsymbol{K} \\ \boldsymbol{I} \end{bmatrix} \right\|_{\mathcal{H}_\infty} \sigma_v \right\}$ is constant. The affine constraints are used to parameterize the observer following the procedures in SLS.[22,32] Further inspired by their work, we choose C as $C \ge 2(1 + \|\boldsymbol{K}\|)\|z\boldsymbol{I} - \boldsymbol{A} + \boldsymbol{K}\|_{\mathcal{H}_2}$ and the estimation error satisfies $\epsilon_A\|\boldsymbol{I} - \boldsymbol{A} + \boldsymbol{K}\|_{\mathcal{H}_\infty} \le 1/2$. Then, the optimal observation performance J_{opt} fulfills

$$J_{opt} \le \epsilon_{1,2}\left\{ \sqrt{2}C\left\{ \left\| \begin{bmatrix} \Phi_A \boldsymbol{B} \\ \boldsymbol{I} \end{bmatrix} \right\|_{\mathcal{H}_\infty} \sigma_u + \left\| \begin{bmatrix} \Phi_A \boldsymbol{K} \\ \boldsymbol{I} \end{bmatrix} \right\|_{\mathcal{H}_\infty} \sigma_v \right\} + 2\|z\boldsymbol{I} - \boldsymbol{A} + \boldsymbol{K}\|_{\mathcal{H}_2}\sigma_v \right\}. \tag{34}$$

This result shows that the performance of the optimal observer based on dynamics estimation has a positive correlation with $\epsilon_{1,2}$. The influence of γ to J_{opt} can be discussed by comparing ϵ_A and ϵ_L. When $\epsilon_A \leq \epsilon_L$, J_{opt} is bounded and related to ϵ_L. When γ increases, ϵ_A increases and $\epsilon_A > \epsilon_L$, then $J_{opt} \sim \mathcal{O}(\gamma)$. Note that the increase of γ does not necessarily lead to $\epsilon_A > \epsilon_L$. However, a small γ leads to small ϵ_A when $\mathcal{H}_{\mathcal{A}}$ is fixed, and the performance of the optimal observer does not depend on estimation error bound.

By introducing (19) into (24), it can be determined whether the observer is needed to be given a finite sample. Moreover, a smaller γ benefits designing a stable observer according to (19) and Theorem 2. The complexity of J_{opt} follows $\mathcal{O}(\gamma/\sqrt{(N)})$ and shows that the decrease of γ and the increase of the number of samples helps with obtaining a better observer performance. It is worth mentioning that (15)–(19) need the values of $\hat{\boldsymbol{A}}$ and $\hat{\boldsymbol{B}}$, which are calculated based on the estimation method. Thus, we cannot obtain $\mathcal{H}_A$ and $\mathcal{H}_B$ before the dynamics estimation method returns the result. After obtaining $\mathcal{H}_A$ and $\mathcal{H}_B$, we can design the observer and determine whether the bound of the observer's performance satisfies the requirement. However, decreasing the parameter makes the estimation method sensitive to the noise in the data and the estimation result fluctuates with the increase of the sample number, as shown and discussed in Section 6. Therefore, we recommend readers select the parameter from a large one to a small one with a search-based method.

6 | NUMERICAL SIMULATIONS

In this section, several numerical simulations are conducted to illustrate the estimation and error bound based on the proposed method and the optimality of the designed observer for an unknown LTI system. We mainly focus on the influence of parameter γ. The simulations are used for showing that

- The biased estimator can provide smaller variance results than an unbiased one when the system is with large-variance noise.
- The proposed error bound is valid for the SVR with different γ and noise variance.
- Larger γ benefits designing an observer whose performance is stable under a different number of samples, since the estimation error variance is smaller.

We consider an open-loop stable LTI system with state and input matrices

$$\boldsymbol{A} = \begin{bmatrix} 0.9 & 0.01 & 0 \\ 0.01 & 0.9 & 0.01 \\ 0 & 0.01 & 0.9 \end{bmatrix}, \boldsymbol{B} = \begin{bmatrix} 1 \\ 1.5 \\ 2 \end{bmatrix}. \tag{35}$$

We also consider an open-loop unstable system, adapted from References 23, as follows

$$\boldsymbol{A} = \begin{bmatrix} 1.01 & 0.01 & 0 \\ 0.01 & 1.01 & 0.01 \\ 0 & 0.01 & 1.01 \end{bmatrix}, \boldsymbol{B} = \begin{bmatrix} 1 \\ 1.5 \\ 2 \end{bmatrix}. \tag{36}$$

In our experiments, we use stochastic input with $\sigma_u = 1$, testing the method's performance under different model noises with $\sigma_w = 0.1$, $\sigma_w = 1$ and $\sigma_w = 10$. For the multi-rollout setup, the rollout length is set to $T_0 = 11$, and we vary the number of rollouts from 10 to 450. Empirically, γ is often chosen to range in $(10^{-3}, 10^{-1})$ for the estimator. Besides, due to the truncation error in computation, unsuitable γ would lead to one of the terms in (12a) equals 0 and cause the solution to fail. We select $\gamma = 0.005$, $\gamma = 0.01$, $\gamma = 0.05$, and $\gamma = 0.1$. LIBSVM is modified[49] with quadratic loss function. For the error bound calculation, we select the matrices bound $M = 1.1$ and possibility coefficient $\delta = 0.01$.

6.1 | Estimation for systems with varying process noise

First, the estimator (12) with $\gamma = 0.05$ is used to estimate the open-loop stable system (35) and open-loop unstable system (36). The sample length used for estimation is set from 100 to 4500 to show the variation of error based on different sample

TABLE 2 RMSEs of estimations based on the OLS method and the proposed method with varying process noises for different systems.

		$\sigma_w = 0.1$		$\sigma_w = 1$		$\sigma_w = 10$	
		OLS	**Ours**	**OLS**	**Ours**	**OLS**	**Ours**
Open-loop stable system (35)	$\tilde{\boldsymbol{A}}$	0.0261	0.0265	0.0328	0.0354	0.0541	**0.0484**
	$\tilde{\boldsymbol{B}}$	0.0029	0.0038	0.0211	0.0315	0.4278	**0.2695**
Open-loop unstable system (36)	$\tilde{\boldsymbol{A}}$	0.0225	0.0236	0.0166	0.0165	0.0171	**0.0168**
	$\tilde{\boldsymbol{B}}$	0.0019	0.0036	0.0374	0.0359	0.3774	**0.2506**

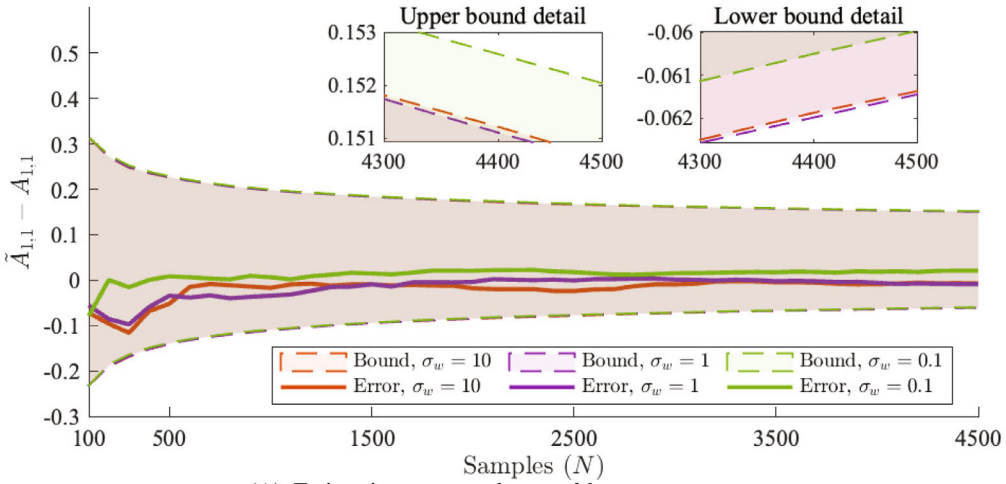

(A) Estimation on open-loop stable system

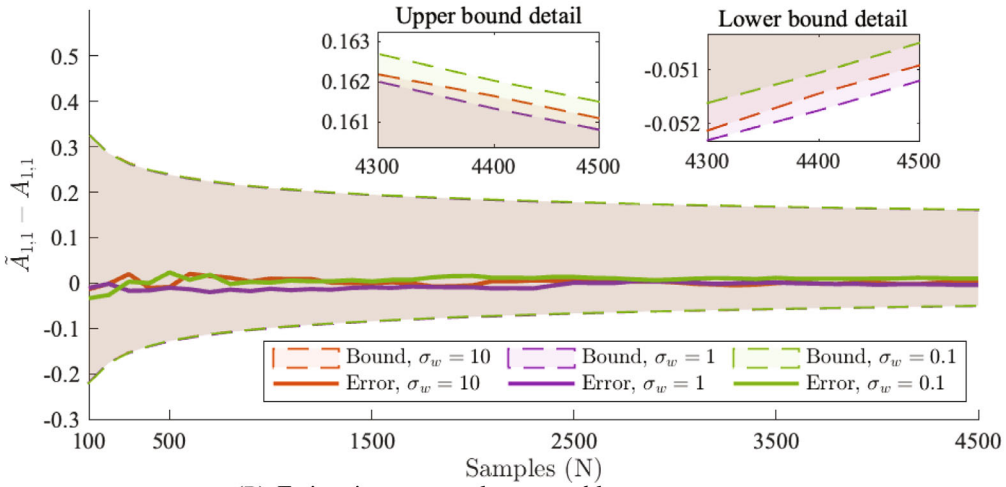

(B) Estimation on open-loop unstable system

FIGURE 2 Estimation based on the proposed method for systems with varying process noise.

numbers. OLS is used to estimate the dynamics based on the same data for a fair comparison. Root mean square error (RMSE) is used to measure the estimation error of $\boldsymbol{A}$, $\boldsymbol{B}$. Table 2 shows the statistical results of 45 repeated estimations. The RMSE of the estimation of the proposed method is smaller than that of OLS when the process noise becomes larger, which is consistent with the theoretical analysis. This illustrates that SVR is more suitable for dynamics estimation with large-variance noise since the lower variance of the error provides less volatile results. The behavior of the proposed estimator with varying process noise is shown in Figure 2. The differences in estimation error on different process noises are small, which shows that the variance of process noise has little effect on the proposed estimator. The error bounds

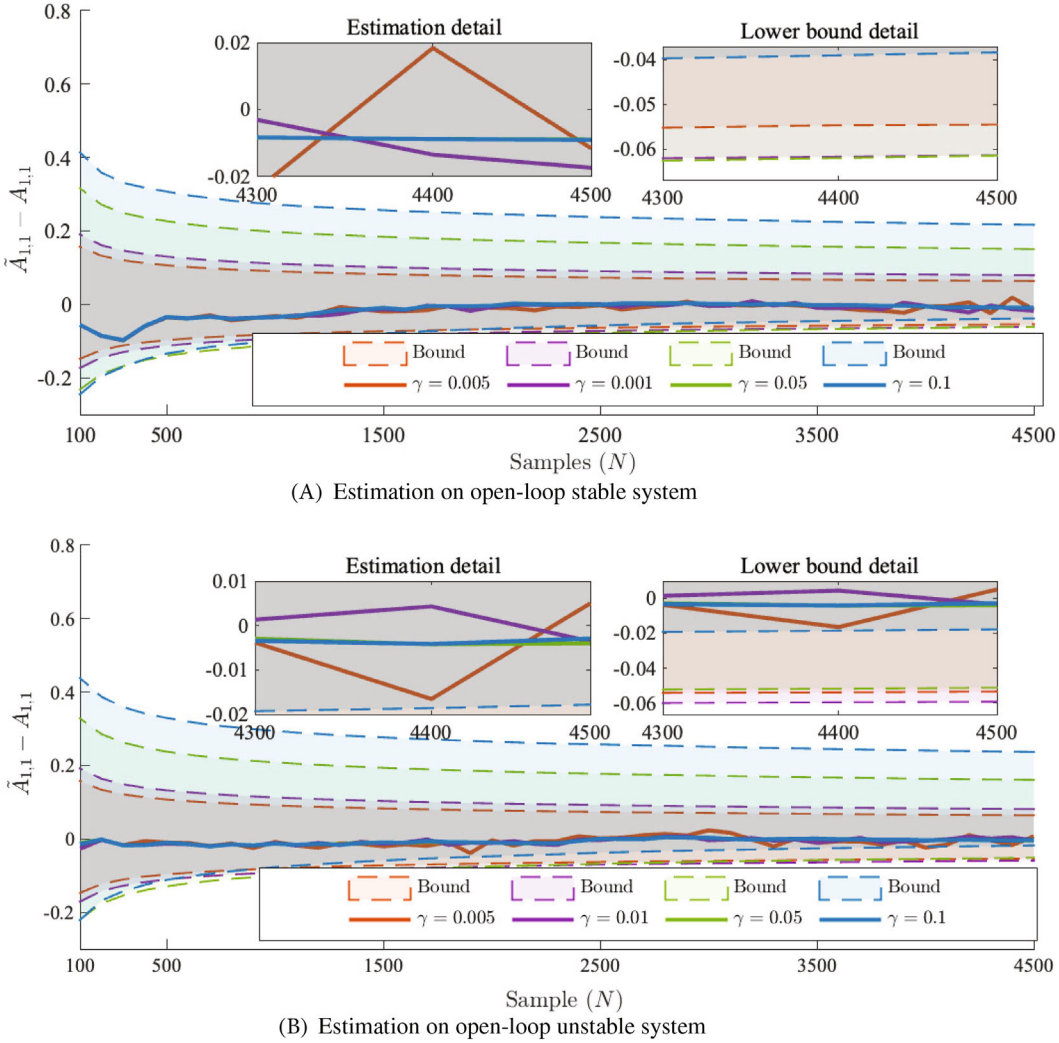

FIGURE 3 Estimation based on the proposed method with varying parameter.

given in (20) are effective. The error intervals tend to be smaller when introducing more samples to the estimation process. Furthermore, the variance of process noise has little effect on error bounds, which shows the robustness of the proposed estimator (12) and validates the error bound analysis (20).

6.2 | Estimation with varying parameter of the proposed estimator

Then, the estimations of the proposed method with varying sample lengths and parameter γ are conducted. The behavior of the proposed estimator is shown in Figure 3. The proposed estimator works well on both open-loop stable and unstable systems. The error upper bounds of estimation significantly change with parameter γ. This is due to the bias-variance trade-off in the proposed method. It cannot be unbiased while holding low variance at the same time. Moreover, as presented in the detail of the lower bound in Figure 3B, the variation of the estimation is large when parameter γ is small. When γ is small, the estimator seeks a smaller biased result, the upper bound is dragged to the x-axis, and the variance increases. The variation of γ also changes the interval between the upper and lower bound. When seeking a small interval of the error bound, it can be done with smaller γ. From the point of stable observer design, we want to have dynamics estimations that do not influence the stability's determination. In Figure 3A, $\boldsymbol{A}$ is determined to be stable after $N = 1800$ for the error bound guarantees $\|\boldsymbol{A}\| < 1$ as (21). Reducing the estimation error interval can be done by introducing more samples into the previous OLS-based estimation methods, whereas the proposed estimator provides two ways (i.e., turning γ and adding samples) to change the interval.

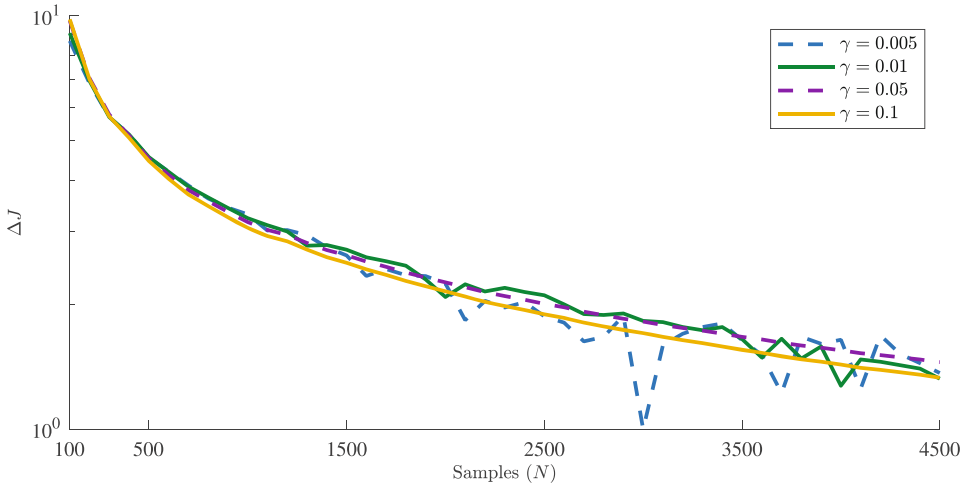

FIGURE 4 Deviation between observer cost bound and cost with different estimation parameter γ on the open-looped stable system.

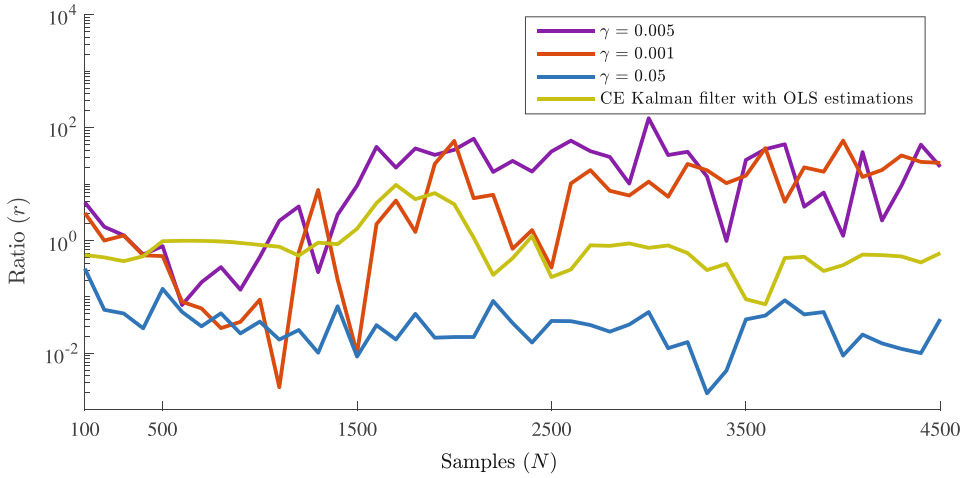

(A) Cost ratio between observers on open-loop stable system

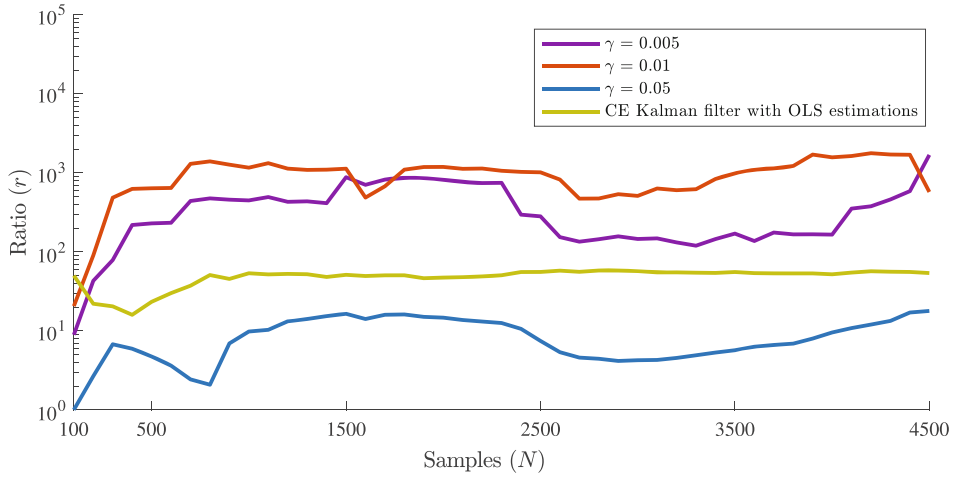

(B) Cost ratio between observers on open-loop unstable system

FIGURE 5 Ratios of observer costs with different estimation parameter γ, where $r := (J_\gamma - J^*)/J^*$, J_γ denotes the cost with different estimation parameter γ, J^* is the benchmark cost with $\gamma = 0.1$.

6.3 | Simulations on observer gain design and observer performance analysis

Based on the estimation results with different γ, the stable observer gain is designed based on Theorem 2. The stable gains are designed based on estimation with sample length from 100 to 4500. We use the same gain if (24) holds.

Then, observers are constructed to verify the proposed cost bound and observer performance based on estimations with different γ. We run 1000 Monte Carlo simulations for different sample lengths N. The mean cost J and cost bound J_b for the observer of the open-loop stable system at each sample length are calculated. The latter is obtained according to Theorem 3 with $\epsilon_1 = \epsilon_B$, for ϵ_B is maximum among the candidates when $N \leq 4500$. The deviation $\Delta J = J_b - J$ at each sample length is shown in Figure 4. Deviations are above 0, which means the cost bound is valid with different γ. Furthermore, costs with different γ are compared in the open-loop stable and unstable systems. In Figure 5, we show the ratios of observer costs with different γ. Ratio $r := (J_\gamma - J^*)/J^*$, where J_γ denotes the cost with different estimation parameter γ, J^* is the benchmark cost with $\gamma = 0.1$. The reason for choosing $\gamma = 0.1$ as the benchmark is that it leads to a good trade-off between bias and variance, resulting in a smaller variance of the cost. This makes it suitable for showing the fluctuations of the different costs and evaluating the performance of the observer under different parameter choices. The proposed observer design procedure provides stable observations for both open-loop stable and unstable systems. It is also clear that the cost variance is much larger when γ is smaller. This corresponds to the high-variation estimation when γ is small. Thus, we recommend using a relatively large γ to have a stable estimation result for a stable observer performance. Certainty–Equivalent (CE) Kalman filters with OLS estimations are also designed to show the performance.[22] The cost ratio $(J_{\text{CE}} - J^*)/J^*$ is shown in Figure 5. The performance fluctuation of the CE-Kalman filter is moderate compared with those of the proposed method. The cost is also moderate, which indicates that the biased estimation method can achieve more flexibility than OLS methods since there is a parameter to trade off the bias and the variance in the SVR.

In conclusion, the simulations demonstrate that the parameter γ of the proposed estimator influences the estimation results and observer performance, and a suitable γ benefits the observer design and stable performance. Empirical speaking, a small γ helps with determining a small estimation bound. A large γ helps with providing a stable estimation result and stable observer performance.

7 | CONCLUSION

This article mainly focused on SVR-based observer design and analysis for unknown linear systems. We showed the detailed system dynamics estimation procedure, including data collection and the estimator's formulation. Furthermore, we analyzed and formulated the sample complexity bounds for the estimation error of the proposed method as $\mathcal{O}(1/\sqrt{N})$ with an adjustable parameter γ, which provides another way to change the estimation error interval besides introducing more samples. We also proposed an observer gain design procedure to guarantee stability based on the dynamics estimation results and the error bound. The procedure reveals that γ helps find a stable gain set by adjusting the estimation error interval. We further analyze the end-to-end sample complexity for the sub-optimal observer for an unknown system. We formulated a mean square observation error bound for estimation and observer design, connecting the estimation error and observer performance. Finally, numerical simulations verify the proposed methods. Simulations also illustrated that the parameter γ of the proposed method influences the estimation results and observer performance, and a suitable γ benefits the observer design and stable performance.

Future directions for research include investigating the influence of the parameter γ on performance variance in estimation and observer (controller) performance. It may be possible to connect the variation with the parameter over a high probability and investigate optimal parameter selection.

CONFLICT OF INTEREST STATEMENT

The authors declare no potential conflict of interest.

DATA AVAILABILITY STATEMENT

Data sharing not applicable to this article as no datasets were generated or analyzed during the current study.

ORCID

Jianping He https://orcid.org/0000-0002-6253-7802

REFERENCES

1. Ouassaid M, Maaroufi M, Cherkaoui M. Observer-based nonlinear control of power system using sliding mode control strategy. *Electr Power Syst Res*. 2012;84(1):135-143. doi:10.1016/j.epsr.2011.10.014
2. Mi Y, Fu Y, Li D, Wang C, Loh PC, Wang P. The sliding mode load frequency control for hybrid power system based on disturbance observer. *Int J Electron Power*. 2016;74:446-452. doi:10.1016/j.ijepes.2015.07.014
3. Na J, Mahyuddin MN, Herrmann G, Ren X, Barber P. Robust adaptive finite-time parameter estimation and control for robotic systems. *Int J Robust Nonliner*. 2015;25(16):3045-3071. doi:10.1002/rnc.3247
4. Zhang X, Ding F. Adaptive parameter estimation for a general dynamical system with unknown states. *Int J Robust Nonliner*. 2020;30(4):1351-1372. doi:10.1002/rnc.4819
5. Ljung L. System identification. *Applied and Numerical Harmonic Analysis*. Boston, MA: Birkhäuser; 1998:163-173.
6. Young P. An instrumental variable method for real-time identification of a noisy process. *Automatica*. 1970;6(2):271-287. doi:10.1016/0005-1098(70)90098-1
7. Chou C, Verhaegen M. Subspace algorithms for the identification of multivariable dynamic errors-in-variables models. *Automatica*. 1997;33(10):1857-1869. doi:10.1016/s0005-1098(97)00092-7
8. Yu C, Chen J, Verhaegen M. Subspace identification of individual systems in a large-scale heterogeneous network. *Automatica*. 2019;109:108517. doi:10.1016/j.automatica.2019.108517
9. Luders G, Narendra K. An adaptive observer and identifier for a linear system. *IEEE Trans Automat Control*. 1973;18(5):496-499. doi:10.1109/TAC.1973.1100369
10. Zhang Q. Adaptive observer for multiple-input-multiple-output (MIMO) linear time-varying systems. *IEEE Trans Automat Control*. 2002;47(3):525-529. doi:10.1109/9.989154
11. Oliva-Fonseca P, Rueda-Escobedo JG, Moreno JA. Fixed-time adaptive observer for linear time-invariant systems. *2016 IEEE 55th Conference on Decision and Control (CDC)*. IEEE; 2016:1267-1272.
12. Carleo G, Troyer M. Solving the quantum many-body problem with artificial neural networks. *Science*. 2017;355(6325):602-606. doi:10.1126/science.aag2302
13. Hagan MT, Demuth HB, Jesús OD. An introduction to the use of neural networks in control systems. *Int J Robust Nonliner*. 2002;12(11):959-985. doi:10.1002/rnc.727
14. Cherkassky V, Ma Y. Practical selection of SVM parameters and noise estimation for SVM regression. *Neural Netw*. 2004;17(1):113-126. doi:10.1016/S0893-6080(03)00169-2
15. Wei C, Luo J, Dai H, Yin Z, Ma W, Yuan J. Globally robust explicit model predictive control of constrained systems exploiting SVM-based approximation. *Int J Robust Nonliner*. 2017;27(16):3000-3027. doi:10.1002/rnc.3726
16. Sadamoto T, Chakrabortty A, Ji I. Fast online reinforcement learning control using state-space dimensionality reduction. *IEEE Trans Control Network*. 2021;8(1):342-353. doi:10.1109/TCNS.2020.3027780
17. Gao W, Jiang ZP. Adaptive optimal output regulation via output-feedback: An adaptive dynamic programing approach. *2016 IEEE 55th Conference on Decision and Control (CDC)*. IEEE; 2016:5845-5850.
18. Wei Q, Song R, Liao Z, Li B, Lewis FL. Discrete-time impulsive adaptive dynamic programming. *IEEE Trans Cybernetics*. 2020;50(10):4293-4306. doi:10.1109/TCYB.2019.2906694
19. Bauer D, Jansson M. Analysis of the asymptotic properties of the MOESP type of subspace algorithms. *Automatica*. 2000;36(4):497-509. doi:10.1016/S0005-1098(99)00174-0
20. Cherkassky V, Shao X, Mulier F, Vapnik V. Model complexity control for regression using VC generalization bounds. *IEEE Trans Neural Network*. 1999;10(5):1075-1089. doi:10.1109/72.788648
21. Chalimourda A, Schölkopf B, Smola AJ. Experimentally optimal ν in support vector regression for different noise models and parameter settings. *Neural Netw*. 2004;17(1):127-141. doi:10.1016/S0893-6080(03)00209-0
22. Tsiamis A, Matni N, Pappas G. Sample complexity of Kalman filtering for unknown systems. In: Bayen AM, Jadbabaie A, Pappas G, et al., eds. *Proceedings of the 2nd Conference on Learning for Dynamics and Control*. Vol 120. PMLR; 2020:435-444.
23. Dean S, Mania H, Matni N, Recht B, Tu S. On the sample complexity of the linear quadratic regulator. *Found Comput Math*. 2019;20(4):633-679. doi:10.1007/s10208-019-09426-y
24. Zheng Y, Furieri L, Kamgarpour M, Li N. Sample complexity of linear quadratic Gaussian (LQG) control for output feedback systems. In: Jadbabaie A, Lygeros J, Pappas GJ, et al., eds. *Proceedings of the 3rd Conference on Learning for Dynamics and Control*. Vol 144. PMLR; 2021:559-570.
25. Fattahi S, Sojoudi S. Sample complexity of block-sparse system identification problem. *IEEE Trans Control Network*. 2021;8(4):1905-1917. doi:10.1109/TCNS.2021.3089141
26. Simchowitz M, Mania H, Tu S, Jordan MI, Recht B. Learning without mixing: towards a sharp analysis of linear system identification. In: Bubeck S, Perchet V, Rigollet P, eds. *Proceedings of the 31st Conference On Learning Theory*. Vol 75. PMLR; 2018:439-473.
27. Sun Y, Oymak S, Fazel M. Finite sample system identification: Optimal rates and the role of regularization. In: Bayen AM, Jadbabaie A, Pappas G, et al., eds. *Proceedings of the 2nd Conference on Learning for Dynamics and Control*. Vol 120. PMLR; 2020:16-25.
28. Oymak S, Ozay N. Revisiting Ho-Kalman based system identification: robustness and finite-sample analysis. *IEEE Trans Automat Control*. 2022;67(4):1914-1928. doi:10.1109/TAC.2021.3083651
29. Sarkar T, Rakhlin A, Dahleh MA. Finite time LTI system identification. *J Mach Learn Res*. 2021;22(1):1186-1246.
30. Simchowitz M, Boczar R, Recht B. Learning linear dynamical systems with semi-parametric least squares. In: Beygelzimer A, Hsu D, eds. *Proceedings of the Thirty-Second Conference on Learning Theory. 99 of Proc. Mach*. PMLR; 2019:2714-2802.

31. Tsiamis A, Pappas GJ. Linear systems can be hard to learn. *2021 60th IEEE Conference on Decision and Control (CDC)*. IEEE; 2021:2903-2910.
32. Wang YS, Matni N, Doyle JC. A system-level approach to controller synthesis. *IEEE Trans Automat Control*. 2019;64(10):4079-4093. doi:10.1109/TAC.2018.2890753
33. Furieri L, Zheng Y, Papachristodoulou A, Kamgarpour M. An input–output parametrization of stabilizing controllers: Amidst Youla and system level synthesis. *IEEE Control Syst Lett*. 2019;3(4):1014-1019. doi:10.1109/LCSYS.2019.2920205
34. Zheng Y, Furieri L, Papachristodoulou A, Li N, Kamgarpour M. On the equivalence of Youla, system-level, and input–output parameterizations. *IEEE Trans Automat Control*. 2021;66(1):413-420. doi:10.1109/TAC.2020.2979785
35. Geman S, Bienenstock E, Doursat R. Neural networks and the bias/variance dilemma. *Neural Comput*. 1992;4(1):1-58. doi:10.1162/neco.1992.4.1.1
36. Valentini G, Dietterich TG. Bias-variance analysis of support vector machines for the development of SVM-based ensemble methods. *J Mach Learn Res*. 2004;5:725-775.
37. Andrews DWK. Stability comparison of estimators. *Econometrica*. 1986;54(5):1207-1235.
38. Anderson PM, Fouad AA. *Power system control and stability*. John Wiley & Sons; 2008.
39. Domínguez-García JL, Ugalde-Loo CE, Bianchi F, Gomis-Bellmunt O. Input–output signal selection for damping of power system oscillations using wind power plants. *Int J Electr Power Energy Syst*. 2014;58:75-84. doi:10.1016/j.ijepes.2014.01.001
40. Rojo-Alvarez J, Martinez-Ramon M, Cumplido dM, Artes-Rodriguez A, Figueiras-Vidal A. Support vector method for robust ARMA system identification. *IEEE Trans Signal Proces*. 2004;52(1):155-164. doi:10.1109/tsp.2003.820084
41. Welch G, Bishop G. *An introduction to the Kalman filter*. Chapel HillChapel Hill, NC: University of North Carolina; 1995.
42. Willems JC, Rapisarda P, Markovsky I, De Moor BL. A note on persistency of excitation. *Syst Control Lett*. 2005;54(4):325-329. doi:10.1016/j.sysconle.2004.09.003
43. Clarke SM, Griebsch JH, Simpson TW. Analysis of support vector regression for approximation of complex engineering analyses. *J Mech Des*. 2004;127(6):1077-1087. doi:10.1115/1.1897403
44. Balas GJ, Doyle JC, Glover K, Packard A, Smith R. *μ-analysis and synthesis toolbox*. The Mathworks, Inc., MA; 1993:434.
45. Hjartarson A, Seiler P, Packard A. LPVTools: A toolbox for modeling, analysis, and synthesis of parameter varying control systems. *IFAC-PapersOnLine*. 2015;48(26):139-145. 1st IFAC Workshop on Linear Parameter Varying Systems LPVS 2015. doi:10.1016/j.ifacol.2015.11.127
46. Doyle J, Glover K, Khargonekar P, Francis B. State-space solutions to standard H_2 and H_∞ control problems. *IEEE Trans Automat Control*. 1989;34(8):831-847. doi:10.1109/9.29425
47. Scherer C. *Theory of Robust Control*. Delft University of Technology; 2001:1-160.
48. Kailath T, Sayed A, Hassibi B. *Linear Estimation*. Prentice-Hall information and system sciences seriesPrentice Hall; 2000.
49. Chang CC, Lin CJ. LIBSVM: a library for support vector machines. *ACM Trans Intell Syst Technol*. 2011;2(3):1-27. doi:10.1145/1961189.1961199
50. Lugosi G, Mendelson S. Sub-Gaussian estimators of the mean of a random vector. *Ann Stat*. 2019;47(2):783-794. doi:10.1214/17-aos1639
51. Vershynin R. Introduction to the non-asymptotic analysis of random matrices. arXiv preprint, arXiv:1011.3027 2010.

How to cite this article: Ding X, Wang H, He J, Chen C, Guan X. On the sample complexity of observers for unknown linear systems with biased dynamics estimations. *Int J Robust Nonlinear Control*. 2023;1-20. doi: 10.1002/rnc.6933

APPENDIX A. PROOFS

A.1 Proof of Lemma 1

First, we give the relationship between SVR and OLS regression results. For clear expression, we use different notations in this section. The standard linear relationship is given as $\boldsymbol{y} = \boldsymbol{a}^\top \boldsymbol{x} + \boldsymbol{b}$, where $\boldsymbol{b} \sim \mathcal{N}(0, \sigma \boldsymbol{I})$. More specifically, the linear operator a in our problem is A. We use a here for a general illustration. The estimation of $\boldsymbol{a}$ is constructed based on $\boldsymbol{y}$ and $\boldsymbol{x}$.

To ease the notation, we use $\boldsymbol{w}$ and $\boldsymbol{v}$ to represent the results of SVR and OLS in this proof, respectively. Note that (12) is the formulation of SVR when it is without magnitude term. The following relationship can be obtained by analysing $\frac{\partial \mathcal{L}}{\partial \boldsymbol{w}} = 0$ according to Reference 40.

$$\boldsymbol{w}_i = \frac{1}{1+\gamma} \boldsymbol{v}_i.$$

This conclusion is also given in Reference 40 by geometrical decomposition of SVR and OLS. Then, the expectation of $\boldsymbol{w}$ is given as

$$\mathbb{E}(\boldsymbol{w}_i) = \mathbb{E}\left(\frac{1}{1+\gamma} \boldsymbol{v}_i\right) = \frac{1}{1+\gamma} \mathbb{E}(\boldsymbol{v}_i) = \frac{1}{1+\gamma} \boldsymbol{a}_i.$$

Note that OLS is an unbiased estimator when the system with Gaussian excitation. Thus, $E(v)$ equals the actual value. The covariance of w is given as

$$\mathbb{V}(\boldsymbol{w}_i) = \frac{1}{1+\gamma}(\mathbb{V}(\boldsymbol{v}_i) + \gamma \boldsymbol{a}_i^2).$$

Recall the covariance of OLS estimation is

$$\mathbb{V}(\boldsymbol{v}) = \sigma(\boldsymbol{x}\boldsymbol{x}^\top)^{-1}.$$

For $\|\boldsymbol{A}\| \le M$ in Assumption. 1, thus, $\|\boldsymbol{a}\| \le M$ in the linear relationship and we have

$$\mathbb{V}(\boldsymbol{w}) \le \frac{1}{1+\gamma}(\sigma(\boldsymbol{x}\boldsymbol{x}^\top)^{-1} + \gamma M^2 \boldsymbol{I}).$$

Lemma 1 stands. It also reveals that the SVR provides a biased estimation, whereas the estimation covariance is smaller than that of OLS when $\mathbb{V}(\boldsymbol{v}_i) \ge \boldsymbol{a}_i^2$.

A.2 Proof of Theorem 1

According to (1.1) of Reference 50, when $\boldsymbol{X}$ follows a normal distribution with mean μ and covariance matrix Σ, then the sample mean $\overline{\mu}$ is also normal with mean μ and covariance matrix $(1/N)\Sigma$, and therefore, for any $0 < \delta < 1$, with probability at least $1 - \delta$

$$\|\overline{\mu} - \mu\| \le \sqrt{\frac{\mathrm{Tr}(\Sigma)}{N}} + \sqrt{\frac{2\lambda_{\max}\log(1/\delta)}{N}},$$

where $\lambda_{\max}$ denotes the largest eigenvalue of Σ. According to the distribution of estimation $\tilde{\boldsymbol{A}}$ given by (15), the nonasymptotic bound of estimation error is given as

$$\begin{aligned}
&\|\tilde{\boldsymbol{A}}_i - E(\tilde{\boldsymbol{A}}_i)\| \\
&\le \sqrt{\frac{\mathrm{Tr}\left[\boldsymbol{\sigma}_A^2(\boldsymbol{y}_{T_0-1}\boldsymbol{y}_{T_0-1}^\top)^{-1}\right] + n\gamma M^2}{(1+\gamma)N_0}} + \sqrt{\frac{2\left\{\mathrm{Tr}\left[\boldsymbol{\sigma}_A^2(\boldsymbol{y}_{T_0-1}\boldsymbol{y}_{T_0-1}^\top)^{-1}\right] + n\gamma M^2\right\}\log(1/\delta)}{(1+\gamma)N_0}} \\
&\le \sqrt{\frac{\theta_A + n\gamma M^2}{(1+\gamma)N_0}} + \sqrt{\frac{2(\theta_A + n\gamma M^2)\log(1/\delta)}{(1+\gamma)N_0}},
\end{aligned} \tag{A1}$$

where $\theta_A = n(mM\sigma_u^2 + \sigma_w^2 + (M+1)\sigma_v^2)\|(\boldsymbol{y}_{T_0-1}\boldsymbol{y}_{T_0-1}^\top)^{-1}\|$ and $N_0 = (T_0 - 1)N$. According to Corollary 5.35 of Reference 51 and Lemma 2.3 of Reference 23, the nonasymptotic bound of $\|(\boldsymbol{y}_{T_0-1}\boldsymbol{y}_{T_0-1}^\top)^{-1}\|$ is given as

$$\|(\boldsymbol{y}_{T_0-1}\boldsymbol{y}\boldsymbol{y}_{T_0-1}^\top)^{-1}\| \le \frac{\|(v v^\top)^{-1}\|}{nM^{2T_0-1}\sigma_u^2 + M^{2T_0-2}(\sigma_w^2 + \sigma_v^2) + M^{2T_0}\sigma_v^2}, \tag{A2}$$

where v is a quantity that follows a standard Gaussian distribution and with probability at least $1 - \delta$,

$$\|(v v^\top)^{-1}\|^{\frac{1}{2}} \le \frac{1}{\sqrt{N} + \sqrt{n} + \sqrt{2\log(1/\delta)}} \le \frac{2}{\sqrt{N}}. \tag{A3}$$

Combine (A2) and (A3), it gets

$$\theta_A \le \frac{4n(mM\sigma_u^2 + \sigma_w^2 + (M+1)\sigma_v^2)}{N(nM^{2T_0-1}\sigma_u^2 + M^{2T_0-2}(\sigma_w^2 + \sigma_v^2) + M^{2T_0}\sigma_v^2)}. \tag{A4}$$

The upper bound is used in (A1) as $\theta_A = \frac{4n(mM\sigma_u^2+\sigma_w^2+(M+1)\sigma_v^2)}{N(nM^{2T_0-1}\sigma_u^2+M^{2T_0-2}(\sigma_w^2+\sigma_v^2)+M^{2T_0}\sigma_v^2)}$, which does not influence the inequality of (A1).

Note that $\tilde{\boldsymbol{A}}_i - E(\tilde{\boldsymbol{A}}_i) = \frac{\gamma}{1+\gamma}\tilde{\boldsymbol{A}}_i - \frac{1}{1+\gamma}\Delta\boldsymbol{A}_i$, and $\|\tilde{\boldsymbol{A}}_i - E(\tilde{\boldsymbol{A}}_i)\| = \frac{1}{1+\gamma}\|\gamma\tilde{\boldsymbol{A}}_i - \Delta\boldsymbol{A}_i\|$. Theorem 1 holds for $\boldsymbol{A}$ estimation. Similarly, the nonasymptotic bound of estimation error of $\tilde{\boldsymbol{B}}_i$ is

$$\|\tilde{\boldsymbol{B}}_i - E(\tilde{\boldsymbol{B}}_i)\| \le \sqrt{\frac{\theta_B + m\gamma M^2}{(1+\gamma)N_0}} + \sqrt{\frac{2(\theta_B + m\gamma M^2)\log(1/\delta)}{(1+\gamma)N_0}}, \tag{A5}$$

where $N_0 = (T_0 - 1)N$, $\theta_B = m(nM^{2T_0-1}\sigma_u^2 + (M^{2T_0-2}+1)\sigma_w^2 + (M+1)\sigma_v^2)\|(\boldsymbol{u}_{T_0-1}\boldsymbol{u}_{T_0-1}^\top)^{-1}\|$ which has the upper bound as

$$\theta_B = \frac{4m(nM^{2T_0-1}\sigma_u^2 + (M^{2T_0-2}+1)\sigma_w^2 + (M+1)\sigma_v^2)}{N\sigma_u^2}. \tag{A6}$$

A.3 Proof of Lemma 2

For each element in $\tilde{\boldsymbol{A}}_i$ and $\Delta\boldsymbol{A}_i$, it has $\|\gamma\tilde{\boldsymbol{A}}_{i,j} - \Delta\boldsymbol{A}_{i,j}\| \le \|\gamma\tilde{\boldsymbol{A}}_i - \Delta\boldsymbol{A}_i\|$. For each elements in $\tilde{\boldsymbol{A}}_i$, it has

$$\Delta\boldsymbol{A}_{i,j}^2 - 2\gamma\tilde{\boldsymbol{A}}_{i,j}\Delta\boldsymbol{A}_{i,j} - (1+\gamma)\mathcal{H}_A + \gamma^2\tilde{\boldsymbol{A}}_{i,j}^2 \le 0, \tag{A7}$$

Since the coefficient of $\Delta\boldsymbol{A}_{i,j}^2$ is 1, the parabola has a minimum point and opens upward. The limit points of $\Delta\overline{\boldsymbol{A}}_{i,j}$ are obtained by solving (A7) as

$$\gamma\tilde{\boldsymbol{A}}_{i,j} \pm \frac{1}{2}\sqrt{4\gamma^2\tilde{\boldsymbol{A}}_{i,j}^2 - 4(\gamma^2\tilde{\boldsymbol{A}}_{i,j}^2 - (1+\gamma)\mathcal{H}_A)} = \gamma\tilde{\boldsymbol{A}}_{i,j} \pm \sqrt{(1+\gamma)\mathcal{H}_A}. \tag{A8}$$

Then,

$$\Delta\boldsymbol{A}_{i,j} \in \mathcal{B}\left(\gamma\tilde{\boldsymbol{A}}_{i,j}, \sqrt{(1+\gamma)\mathcal{H}_A}\right).$$

The interval of $\Delta\boldsymbol{B}_{i,j}$ can be obtained based the similar manipulations of that of $\Delta\boldsymbol{A}_{i,j}$.

A.4 Proof of Theorem 2

The main idea of designing a stable observer gain is to keep the eigenvalue less than 1. Here we adapt a conservative Gershgorin circle theorem for a general form of matrix $\boldsymbol{A} - \boldsymbol{LC}$.

The center of the disc of each row is $\|\boldsymbol{A}_{i,i} - \{\boldsymbol{LC}\}_{i,j}\|$, which is in a unit circle. The largest radius of the disc is $\|(1+\gamma)\tilde{\boldsymbol{A}}_{i,j} - \{\boldsymbol{LC}\}_{i,j}\| + \sqrt{(1+\gamma)\mathcal{H}_A}$. The condition is obvious when the disc is in the unit circle.

A.5 Proof of Theorem 3

According to Lemma 4, it has

$$J = \left\| \begin{bmatrix}\tilde{\Phi}_w & \tilde{\Phi}_v\end{bmatrix} \begin{bmatrix}\boldsymbol{K} \\ -\boldsymbol{I}\end{bmatrix} \sigma_v + \tilde{\Phi}_w[\Delta\boldsymbol{A} \quad \Delta\boldsymbol{L}] \begin{bmatrix}\Phi_A\boldsymbol{K} \\ \boldsymbol{I}\end{bmatrix} \sigma_v + \tilde{\Phi}_w[\Delta\boldsymbol{A} \quad \Delta\boldsymbol{B}] \begin{bmatrix}\Phi_A\boldsymbol{B} \\ \boldsymbol{I}\end{bmatrix} \sigma_u \right\|_{\mathcal{H}_2}, \tag{A9}$$

Inspired by Lemma 2 of Reference 22 and Proposition 3.5 of Reference 23, the inequality is

$$\begin{aligned} J &\le \left\| \begin{bmatrix}\tilde{\Phi}_w & \tilde{\Phi}_v\end{bmatrix} \begin{bmatrix}\boldsymbol{K} \\ -\boldsymbol{I}\end{bmatrix} \sigma_v \right\|_{\mathcal{H}_2} + \left\| \tilde{\Phi}_w[\Delta\boldsymbol{A} \quad \Delta\boldsymbol{B}] \begin{bmatrix}\Phi_A\boldsymbol{B} \\ \boldsymbol{I}\end{bmatrix} \sigma_u \right\|_{\mathcal{H}_2} + \left\| \tilde{\Phi}_w[\Delta\boldsymbol{A} \quad \Delta\boldsymbol{L}] \begin{bmatrix}\Phi_A\boldsymbol{K} \\ \boldsymbol{I}\end{bmatrix} \sigma_v \right\|_{\mathcal{H}_2} \\ &\le \left\|\tilde{\Phi}_w\boldsymbol{K} - \tilde{\Phi}_v\right]\right\|_{\mathcal{H}_2}\sigma_v + \left\|\tilde{\Phi}_w[\Delta\boldsymbol{A} \quad \Delta\boldsymbol{B}]\right\|_{\mathcal{H}_2} \left\| \begin{bmatrix}\Phi_A\boldsymbol{B} \\ \boldsymbol{I}\end{bmatrix} \right\|_{\mathcal{H}_\infty} \sigma_u + \left\|\tilde{\Phi}_w[\Delta\boldsymbol{A} \quad \Delta\boldsymbol{L}]\right\|_{\mathcal{H}_2} \left\| \begin{bmatrix}\Phi_A\boldsymbol{K} \\ \boldsymbol{I}\end{bmatrix} \right\|_{\mathcal{H}_\infty} \sigma_v. \end{aligned} \tag{A10}$$

Since $\|\Delta\boldsymbol{A}\| \le \epsilon_A$, $\|\Delta\boldsymbol{B}\| \le \epsilon_B$, $\|\Delta\boldsymbol{L}\| \le \epsilon_L$, $\epsilon_1 = \max\{\epsilon_A, \epsilon_B\}$ and $\epsilon_2 = \max\{\epsilon_A, \epsilon_L\}$, it has

$$J \le \left\|\tilde{\Phi}_w\boldsymbol{K} - \tilde{\Phi}_v\right]\right\|_{\mathcal{H}_2}\sigma_v + \sqrt{2}\epsilon_1\left\|\tilde{\Phi}_w\right\|_{\mathcal{H}_2} \left\| \begin{bmatrix}\Phi_A\boldsymbol{B} \\ \boldsymbol{I}\end{bmatrix} \right\|_{\mathcal{H}_\infty} \sigma_u + \sqrt{2}\epsilon_2\left\|\tilde{\Phi}_w\right\|_{\mathcal{H}_2} \left\| \begin{bmatrix}\Phi_A\boldsymbol{K} \\ \boldsymbol{I}\end{bmatrix} \right\|_{\mathcal{H}_\infty} \sigma_v. \tag{A11}$$